Q. J. R. Meteorol. Soc. (2000), **126**, pp. 2241–2264

Impact of initial conditions on seasonal simulations with an atmospheric general circulation model

By JEFFREY L. ANDERSON* and JEFFREY J. PLOSHAY
Geophysical Fluid Dynamics Laboratory, USA

(Received 1 March 1999; revised 1 October 1999)

SUMMARY

Many previous studies have examined the use of very long integrations of atmospheric general circulation models (AGCMs) forced by observed sea surface temperatures (SSTs) as proxies for seasonal atmospheric predictions. These long simulations explore a boundary-value problem in which significant deviations from the model's long-term climatology must be a result of the SST forcing. Seasonal lead simulations starting with observed initial conditions (ICs) for the atmosphere and land surface while retaining observed SST forcing are an intermediate step between the pure boundary-value problem and the pure initial-value forecast problem in which SSTs are also predicted. As part of the Dynamical Seasonal Prediction (DSP) experiment, an ensemble of AGCM integrations with observed atmospheric ICs and model climatology land surface ICs was integrated from mid-December through March for 16 years. These DSP simulation ensembles are compared to ensembles of long boundary-value simulations from the same AGCM in a perfect-model setting (no comparisons of simulations to observations are attempted). Significant differences must be due to the impact of the DSP ICs. Surprisingly large and long-lived differences are found in both the mean and the variance of the ensembles. Many appear to occur because the ICs of the DSP runs are inconsistent with the AGCM climatology; an extended period of model 'spin-up' is the result. Some differences are related to local impacts of the land surface ICs while others, like shifts in the distribution of tropical precipitation and a cooling of the northern hemisphere, are less obviously related to the ICs. The results suggest that care will be needed when inserting observed ICs into seasonal predictions in order to avoid the long-term effects of model spin-up.

KEYWORDS: Ensembles Predictability Seasonal forecasting

1. INTRODUCTION

The global impacts of the 1997–98 El-Niño event have provided renewed motivation for investigating the use of numerical models for seasonal predictions of climate, both in the tropics and mid latitudes. Because of difficulties currently associated with fully coupled ocean–atmosphere general circulation models (GCMs), much of the research and most of the operational forecasts for seasonal lead times have been produced using atmospheric GCMs (AGCMs) forced by specified sea surface temperatures (SSTs).

The Atmospheric Model Intercomparison Project (AMIP; Gates 1992), assembled long simulations from many GCMs forced by observed SSTs. In addition to allowing a comparison of model capabilities in general, these simulations have been interpreted as approximate upper bounds on the seasonal-prediction skill that one could obtain when faced with the reality of predicting, rather than using observed, SSTs (Livezey *et al.* 1996). Many operational seasonal-prediction centres have also used AGCMs forced by specified SSTs (Ji *et al.* 1998). In these cases, the SSTs are predictions derived using simpler statistical or numerical models; this methodology has been termed 'two-tiered' prediction.

Recently, several large experiments, e.g. Dynamical Seasonal Prediction (DSP) and PRediction Of climate Variations On Seasonal to interannual Time-scales (PROVOST), have investigated seasonal predictability including the impact of initial conditions (ICs) on seasonal prediction (Shukla *et al.* 2000; Carson 1998; Branković and Palmer 2000; Graham *et al.* 2000). In AMIP simulations, the ICs are so far in the past that they are generally assumed to have no direct impact on the statistics of an ensemble of simulations. Many seasonal-prediction systems have also assumed that the impact of

* Corresponding author: US Department of Commerce, National Oceanic and Atmospheric Administration, Environmental Research Laboratories, Geophysical Fluid Dynamics Laboratory, Princeton University, PO Box 308, Princeton, NJ 08542, USA.

atmospheric and land surface ICs is negligible compared with that of boundary forcing. On the other hand, most other operational AGCM predictions are for relatively short forecast lead times and are predicated on the idea that atmospheric, and to a lesser extent land surface, ICs provide almost all the information needed for the forecast, while the details of SST forcing are mostly irrelevant. At some intermediate time, the short-range prediction initial-value problem and the seasonal-prediction boundary-value problem must overlap, leading to forecast lead times for which both initial and boundary conditions are important to AGCM predictions. There is evidence that SST boundary forcing begins to have an impact on AGCM predictions by approximately ten-day lead times (Mo and Kalnay 1991; Barsugli *et al.* 1999). There is also evidence that ICs still impact AGCM prediction through at least a month (Nogues-Paegle *et al.* 1992; White *et al.* 1993).

Here, the impact of ICs on seasonal lead AGCM simulations is investigated by exploring the differences between AMIP-type simulations (hereafter referred to as AMIP simulations, although these were not official entrants in any US Department of Energy AMIP projects) that are assumed to have lost all relevant dependence on ICs, and seasonal simulations from the DSP experiment in which the AGCM is forced by observed SSTs but started from observed atmospheric ICs and specified land surface ICs. Differences in the mean and the internal variance are examined, focusing on forecast lead times of one half to 3.5 months. Significant differences are attributed to the impact of the ICs on the DSP simulations. Results are discussed in a perfect-model context in which the AGCM is assumed to have no error; a study of the differences in AMIP and DSP skill in simulating the observed atmosphere would be an interesting extension but is not included.

The boundary-forced AGCM is believed to be ergodic, so statistics of the DSP and AMIP ensembles should become indistinguishable if the DSP simulations are extended for a long time; initially, however, the impact of the ICs causes the statistics to be different. The size and longevity of differences in the ensemble mean are of particular interest. In order for ICs to improve traditional measures of simulation skill, the DSP ensemble means must be significantly different from the AMIP ensemble means. If these differences are not large, the motivation for using ICs is gone.

Examining the impact of the ICs on the ensemble variance is also important, because the internal variance, or spread (Barker 1991), is often used to measure the 'potential predictability' of a quantity (Stern and Miyakoda 1995; Rowell 1998; but also see Wobus and Kalnay 1995). It is often assumed that small internal variance in an ensemble implies a fairly confident prediction, while large variance implies large uncertainty. A priori predictions of skill in operational forecasts (Tracton and Kalnay 1993; Buizza and Palmer 1998), in AMIP-type simulations (Ebisuzaki 1995; Chen and van den Dool 1997) and in long initial/boundary-value integrations (Branković *et al.* 1994) have been somewhat disappointing, with correlations of spread measures with skill generally being very small. Nevertheless, some measure of variance should be an increasingly good predictor of the expected skill of a prediction/simulation as models are improved. Throughout this study, the term 'potential predictability' is used in this perfect-model context to refer to the internal variance of the ensemble (see Wittrock and Ripley (1999) for predictability of land surface values). Improved perfect-model potential predictability is not necessarily correlated with improved prediction skill.

Naive intuition might suggest that adding information from accurately observed ICs in the DSP simulations should increase potential predictability. However, this is inconsistent with many previous studies of the insertion of observed ICs into forecast models. A recurring theme is that inserting ICs that do not satisfy a number of model

'balance' conditions leads to a transient period of adjustment (or 'spin-up'), during which there may be a large growth of unbalanced error in the model. Unbalanced ICs inserted into the DSP simulation could, in fact, lead to ensembles with significantly larger variance than is found in the AMIP simulations. The existence of instances of significantly more variance in DSP than in AMIP ensembles would imply that a large spin-up error is occurring in the DSP simulations.

Unfortunately, the interpretation of many seasonal simulation and prediction results is complicated by the fact that land surface and, in some cases, sea ice models have traditionally been treated as integral parts of AGCMs, rather than as separate models like the ocean. Much of the discussion that follows implicitly assumes that the land surface model is part of the AGCM. Observations of soil moisture, soil temperature, snow depth and extent (and other quantities needed for more advanced land surface models) are extremely sparse (Vinnikov *et al.* 1999). It is not clear whether these land surface properties are more appropriately treated as ICs or boundary conditions (like SST) for seasonal-prediction research. Given the dearth of available observations that would allow the land surface properties to be specified like the SSTs, the DSP experiments have chosen only to specify these as ICs; DSP participants are free to choose these ICs as they see fit. Since relatively slow time-scales are associated with many land surface properties, the primary impact of ICs on DSP simulations may come from the ICs for these fields, rather than from ICs for the free atmosphere. Analysis of the results is even more complex, because some land surface processes actually occur on time-scales comparable with those of the atmosphere, for instance the thermal balance in the upper layers of the soil.

The land surface ICs for the DSP experiments discussed here come from a climatological monthly mean from a long forced integration of a previous version of the AGCM. Identical land surface ICs are used in every ensemble member; only the atmospheric ICs vary between ensemble members. Ideally, one would have used observed land surface ICs and sampled the uncertainty in these observations in the ensemble, but this is extremely difficult for available direct land surface observations. If the land surface ICs used for the DSP are no less compatible with the AMIP model's climatology than the available observed ICs, the differences between DSP and AMIP simulations can be viewed as a rough upper bound on the impacts of using observed land surface ICs. Discussion in later sections will address the difficult question of the relative quality of the land surface ICs used for DSP here, and available observed land surface ICs.

Section 2 describes the AGCM used in the AMIP and DSP simulations, the SSTs used for boundary forcing, and the ICs used in the DSP simulations. Section 3 examines differences between the AMIP and DSP simulations over several regions where large differences are found. Section 4 discusses the implications of these results for two-tiered and fully coupled GCM seasonal predictions, and section 5 summarizes and concludes.

2. Model and experimental design

(a) *AGCM*

All integrations described here are made with the same AGCM, the Geophysical Fluid Dynamics Laboratory Experimental Prediction GCM version V197 (Shukla *et al.* 2000). The atmospheric component is a global spectral GCM with T42 truncation (approximately 2.8° by 2.8°) and 18 sigma levels in the vertical (Gordon and Stern 1982). Physical parametrizations include: orographic gravity-wave drag; large-scale condensation; relaxed Arakawa–Schubert (RAS) convection scheme; shallow convection; cloud prediction (interactive with radiation, Gordon (1992)); radiative transfer (2 h averaged),

which varies seasonally; stability dependent vertical eddy fluxes of heat, momentum, and moisture throughout the surface layer, planetary boundary layer, and free atmosphere ('E' physics as described in Sirutis and Miyakoda (1990)); and horizontal diffusion. Orography has been treated by a Gibbs oscillation reduction method (Navarra *et al.* 1994). This model, with simpler physics and varying resolutions, has been shown to be viable for extended-range prediction at the monthly time-scale (Stern and Miyakoda 1989), although systematic biases still contribute significantly to the error fields. Stern and Miyakoda (1995) used a global SST dataset to force an ensemble of AGCM integrations (referred to as AMIP-1 integrations). The potential predictability of seasonal variations in the extratropics by versions of this AGCM has been examined extensively through various approaches (Anderson 1996; Anderson and Stern 1996; Yang *et al.* 1998).

The land surface is a 3-layer model for the purposes of heat conduction, with the lowest level set to a climatological mean temperature at each grid point (Delsol *et al.* 1971). Heat capacity is a function of the soil moisture using the scheme of Deardorf (1978). Land surface hydrology is modelled by a 3-level bucket, with the lowest bucket level set to a climatological mean value at each grid point (ECMWF 1988). Land surface parametrizations include snow cover, which affects albedo and interacts with both the thermal and hydrologic condition of the top level of the soil. Snow is accumulated over sea ice and land points, and disappears if the underlying ice melts.

(*b*) *AMIP simulations*

An ensemble of six AMIP simulations was produced by integrating the AGCM from 1 January 1979 through to the end of 1995. Atmospheric ICs were taken from National Centers for Environmental Prediction (NCEP) re-analyses for 1 to 6 January 1979; each analysis was used as an IC, as if it was the analysis for 1 January 1979. Soil moisture and snow cover ICs were the January climatology from an ensemble of AMIP runs from an earlier version of the AGCM, that was an official entrant in the AMIP-1 experiments (Gates 1992; Stern and Miyakoda 1995), using the procedure discussed in the next subsection. Monthly means from January, February, and March are examined in this study.

Boundary SSTs are created using version 3.1.6 of the ocean data assimilation method of Derber and Rosati (1989) and Rosati *et al.* (1995), which was used to produce coupled GCM forecasts in Rosati *et al.* (1997). After 1982, this version of the data assimilation produces SSTs in which the assimilated SST data lags the real world by approximately 10 days. In regions with strong seasonal cycles of SST, this leads to some differences between this SST forcing and that used for the DSP integrations. Differences are generally less than a tenth of a degree in the tropics and a few tenths in the extratropics.

(*c*) *DSP simulations*

An ensemble of ten DSP integrations was created starting on 15 December for each of the years from 1979 to 1994 (Shukla *et al.* 2000). These simulations extend for 3.5 months to the end of March in the following year, and are referenced by the forecast year for the January (1980 through 1995). Atmospheric ICs for a given year are taken from NCEP re-analysis fields at 12 h intervals from 0000 UTC 13 December to 1200 UTC 17 December, each treated as if it were the state at 1200 UTC 15 December. Although the first 16 days of the ensembles are examined to understand the initial evolution of the DSP ensembles, analysis focuses on monthly means for January, February and March.

The SST forcing is from the Reynolds optimal interpolation dataset (Reynolds and Smith 1994) that was used in all the DSP experiments. As noted above, there are small differences between the SSTs used in the AMIP simulations and these Reynolds SSTs before 1982, and slightly larger differences thereafter. These differences are sufficiently small to appear to have little impact on the results (see section 4).

Soil moisture and snow cover ICs are from the December climatology of the AMIP-1 version of the AGCM (see above). The AMIP-1 model used a single-level bucket to model land surface hydrology, so a single value of soil moisture between 0 and 15 cm is available for the IC. This value is inserted into the top level of the 3-level bucket, the bottom level is set to the specified climatological mean value, and the middle bucket level is set to the average of the top and bottom. The AMIP-1 model was forced with the official AMIP SST dataset from 1 January 1979 to 31 December 1988, and the December climatology was the mean of the last nine Decembers (1980–1988). The AMIP-1 SSTs are very similar over this period to the SST datasets used to force the AMIP-2 simulations discussed in detail here.

Numerical difficulties, resulting from inconsistencies between climatological snow cover and soil temperature conditions, make it difficult to insert AMIP-1 climatological land surface temperatures as ICs for the DSP integrations. Instead, the initial soil temperature is set through an iterative procedure. A single pass of the AGCM's radiation code is performed using a value of 290 K for the atmospheric surface temperature, T_s, at all land points, and a new value of T_s is computed at each point. This procedure is repeated and another updated T_s is computed at each point. Following this, the AGCM is integrated for five time steps with no heat conduction through the soil layers. Finally, the values for the top and middle soil layer temperatures are linearly interpolated between T_s and the climatologically specified temperature (Crutcher and Meserve 1970) of the lowest soil layer. The resulting soil temperature ICs are identical in all ten of the DSP members for each year.

3. Differences between AMIP and DSP simulations

Several key differences between the AMIP and DSP simulations are discussed in this section, focusing first on several regions and then examining hemispheric differences in upper-level fields. In each case, discussion begins with differences in the ensemble-mean fields, and progresses to differences in the ensemble variance.

Differences in the 16-year ensemble means of the DSP and AMIP simulations are examined for January through March; DSP and AMIP values are the mean of 160 and 96 individual monthly means respectively. An unequal-variance t-test (Press *et al.* 1986) is applied to evaluate the significance of the differences in the means of the DSP and AMIP sample distributions. Since the AMIP and DSP distributions are often quite different and non-Gaussian (see for example Figs. 8–10), these significance values must be regarded as loose approximations. In general, only areas where the means are different at the 99% confidence level are shown in figures.

The ratio of the internal variance (Rowell 1998) of the DSP ensembles to that for the AMIP ensembles is also examined. This is computed by first removing the ensemble mean for a given year from the individual ensemble members from that year. The variance of the resulting distributions of anomalies from the ensemble mean are then computed. An f-test (Press *et al.* 1986) is performed on these sample distributions to evaluate the significance of differences in the variance. Since internal variance is often used as a measure of potential predictability in ensembles, this ratio gives a rough idea of the relative potential predictability in the DSP and AMIP simulations. The difference

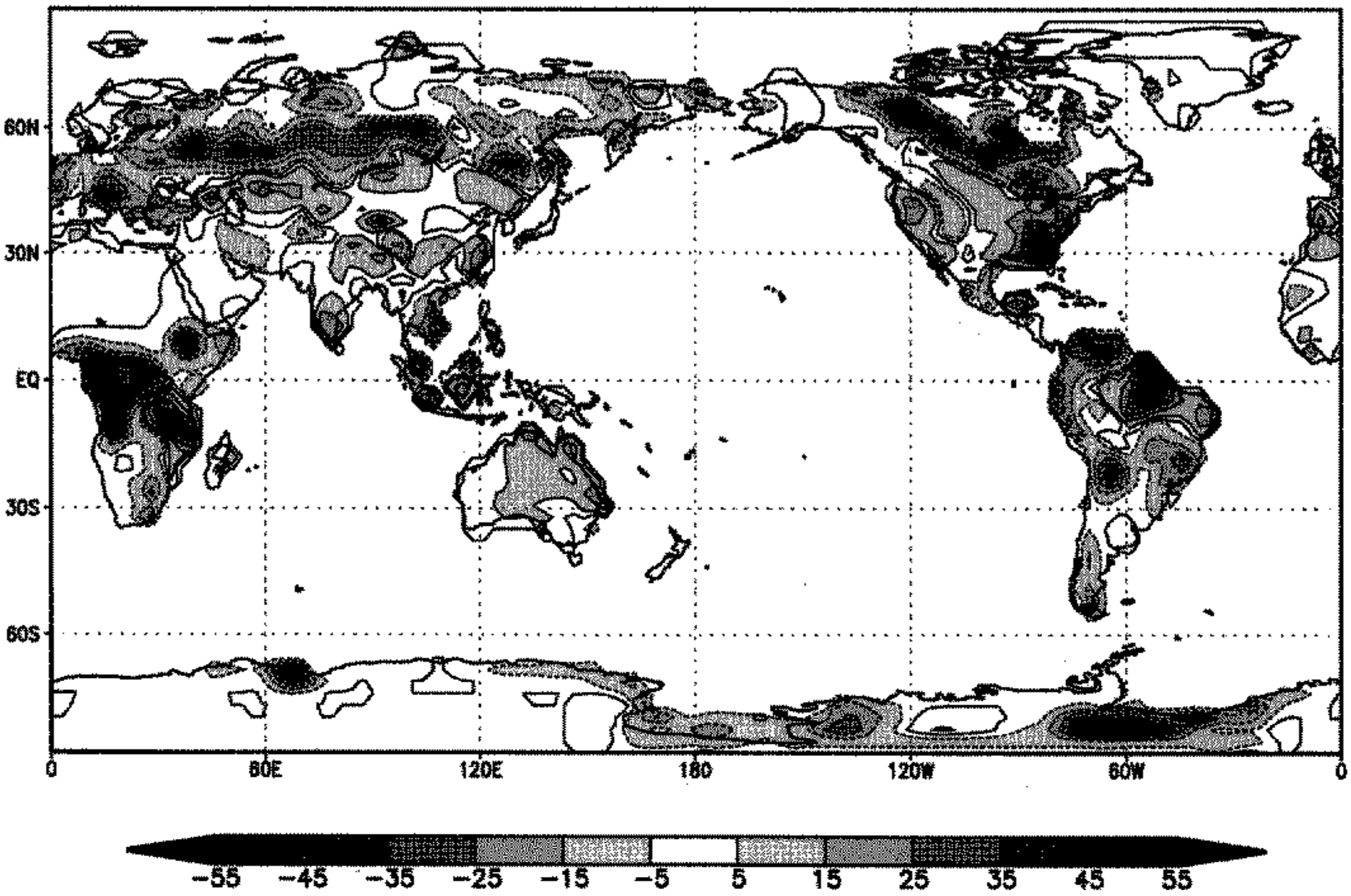

Figure 1. Difference (mm) between Dynamical Seasonal Prediction experiment soil moisture initial conditions and the 1979–95 December climatology from the Atmospheric Model Intercomparison Project simulations; negative contours are dashed.

in sample size (160 versus 96) in the variance computations could conceivably lead to spurious differences in variance. However, estimates of sample variance are quite stable for samples as large as 96; repeating the results with only six ensemble members selected from the DSP set led to no significant differences in any of the figures or results discussed. Figures only display the variance ratio where the confidence level of the f-test exceeds 99%.

Differences in the interannual variability between the DSP and AMIP simulations are not discussed. A comparison of the results from Shukla *et al.* (2000) with similar analyses of the AMIP simulations, suggests that differences in interannual variability are not large; future work will further explore this issue.

(*a*) *Central Africa*

Central Africa is discussed first because differences between the AMIP and DSP simulations appear to be due primarily to direct impacts of the local land surface ICs.

Figure 1 shows differences between the DSP soil moisture ICs (the December climatology from the old AMIP-1 AGCM) and the December climatology from the AMIP simulations. The DSP ICs are much less than the AMIP climatology across much of central Africa, with soil moisture near zero in much of this region in the DSP ICs; this condition persists into January (Fig. 4(a)). From the first few days of the DSP integrations, precipitation is greatly reduced relative to the AMIP integrations over these regions of dry soil, apparently as a direct response to the local supply of water to the atmosphere (Schar *et al.* 1999); this behaviour continues into later months and can be seen in the January mean precipitation differences in Fig. 2(a). This is also reflected in the sharp reduction in the 850 hPa mixing ratio (q850 hereafter) in the DSP simulations

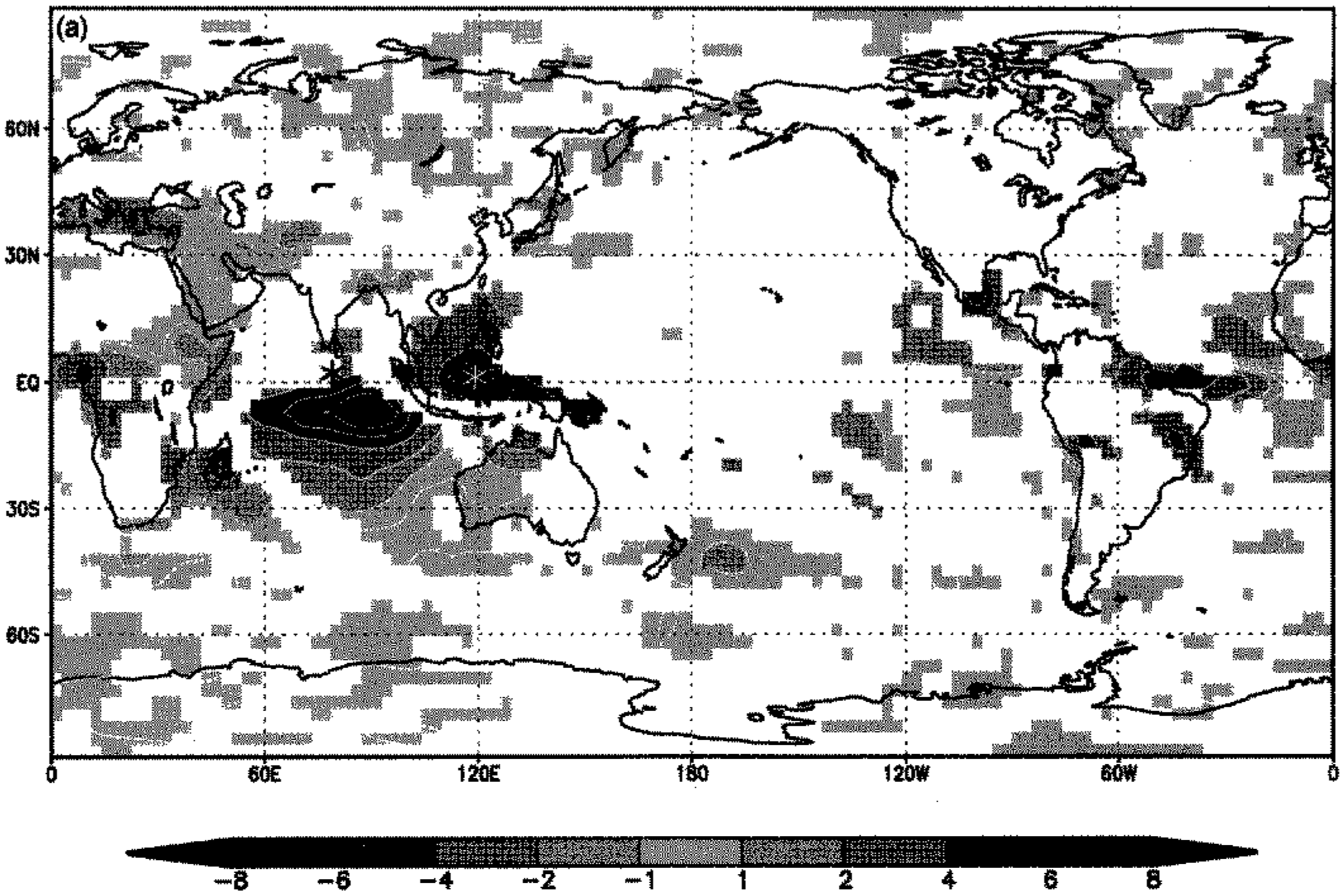

Figure 2. Differences (mm day^{-1}) between the 1980–95 mean ensemble mean precipitation for the Dynamical Seasonal Prediction experiment simulations and the Atmospheric Model Intercomparison Project simulations for: (a) January, and (b) March. Negative contours are dashed, and only regions where an unequal-variance t-test indicates that the difference is significant at greater than 99% confidence are shaded and contoured. The dark (light) asterisk in (a) marks the point examined in detail in Fig. 9 (Fig. 10).

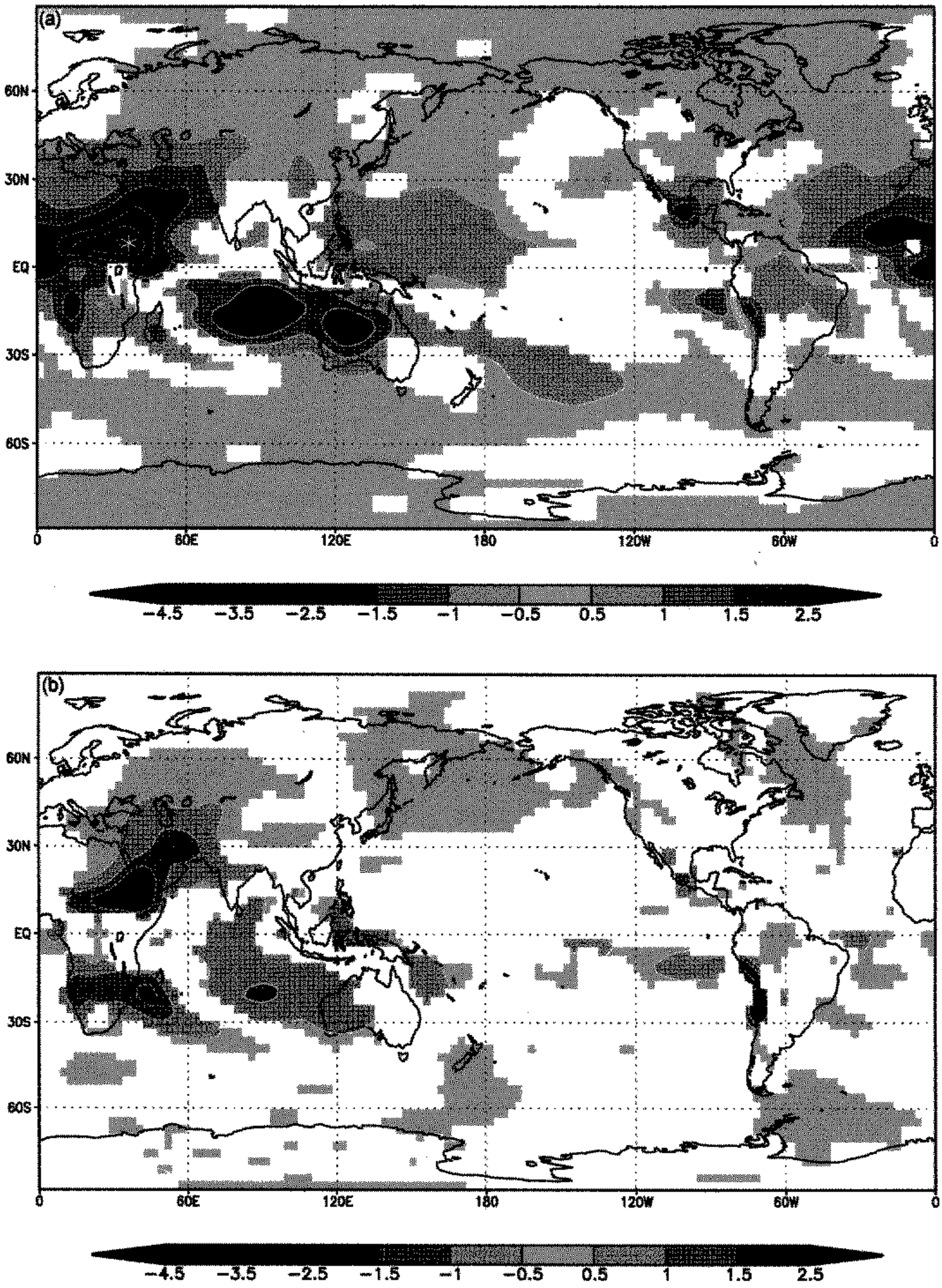

Figure 3. As Fig. 2 but for the 850 hPa mixing ratio (g kg^{-1}). The asterisk in (a) marks the position of the point examined in detail in Fig. 8.

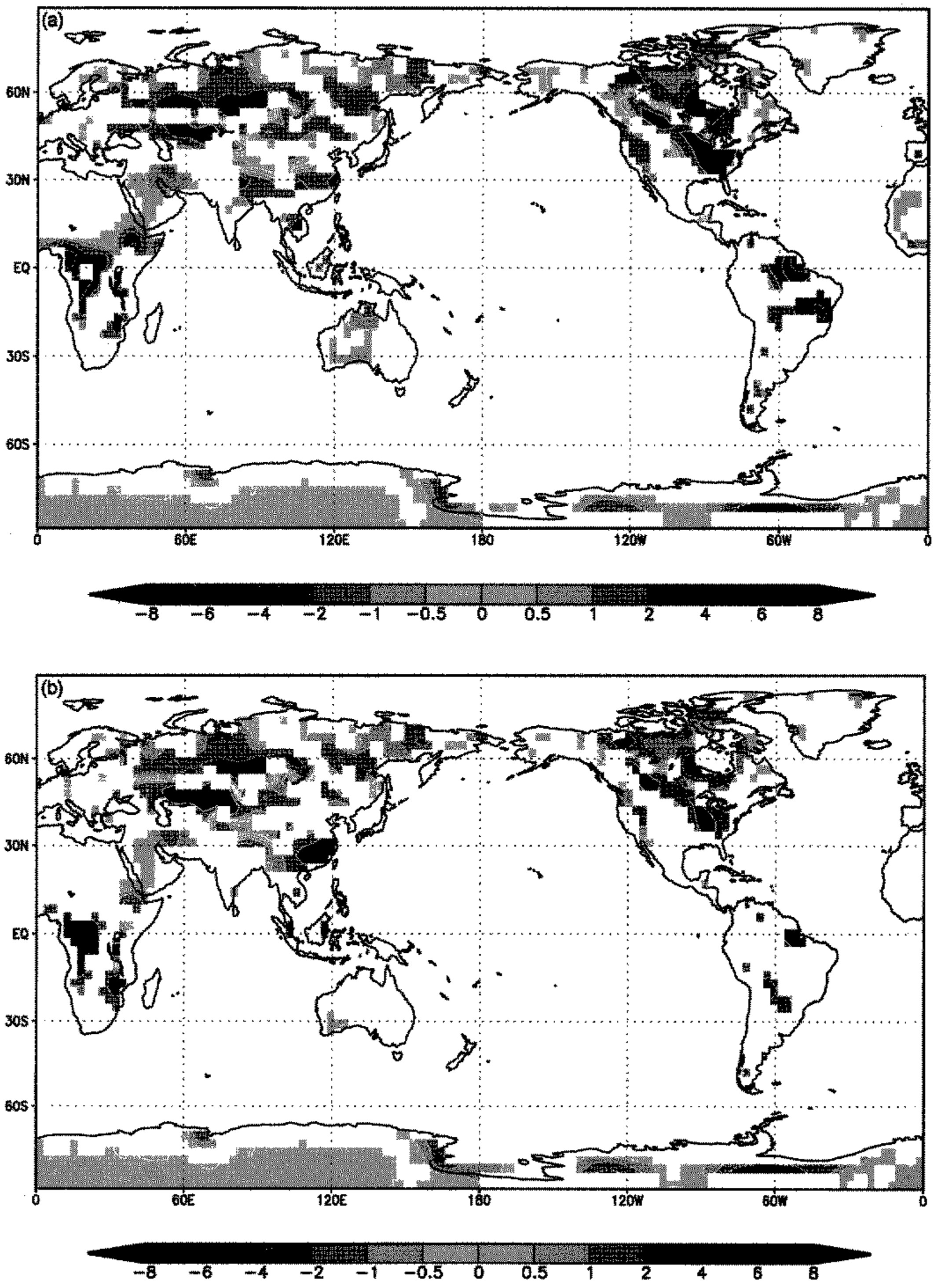

Figure 4. As Fig. 2 but for the soil moisture (cm).

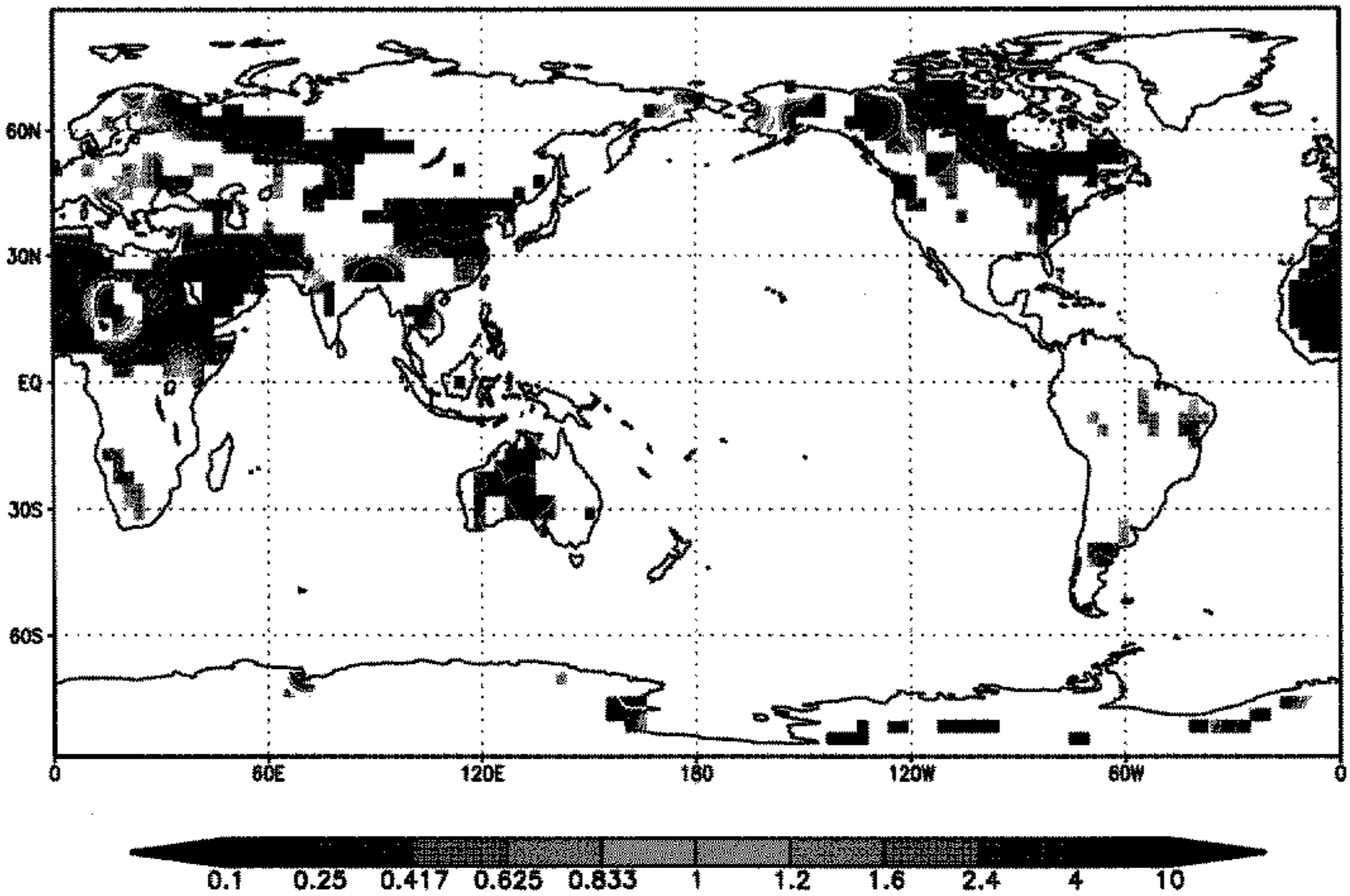

Figure 5. Ratio of Dynamical Seasonal Prediction experiment to Atmospheric Model Intercomparison Project variance of soil moisture around the corresponding ensemble mean (internal variance; see text for details) for January. Contours less than unity are dashed and only regions where an f-test indicates that the difference in variance is significant at greater than 99% confidence are shaded and contoured.

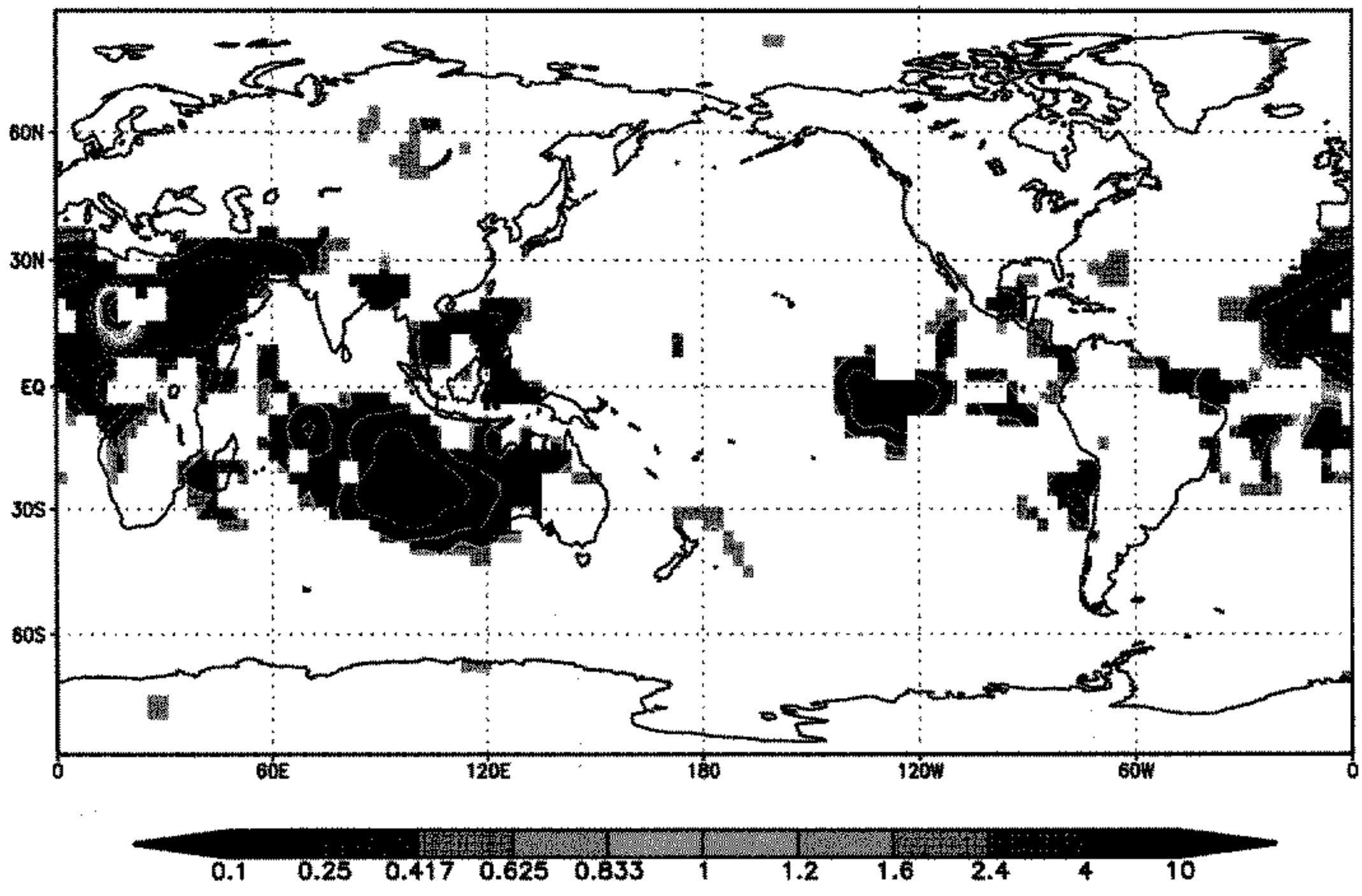

Figure 6. As Fig. 5 but for the precipitation.

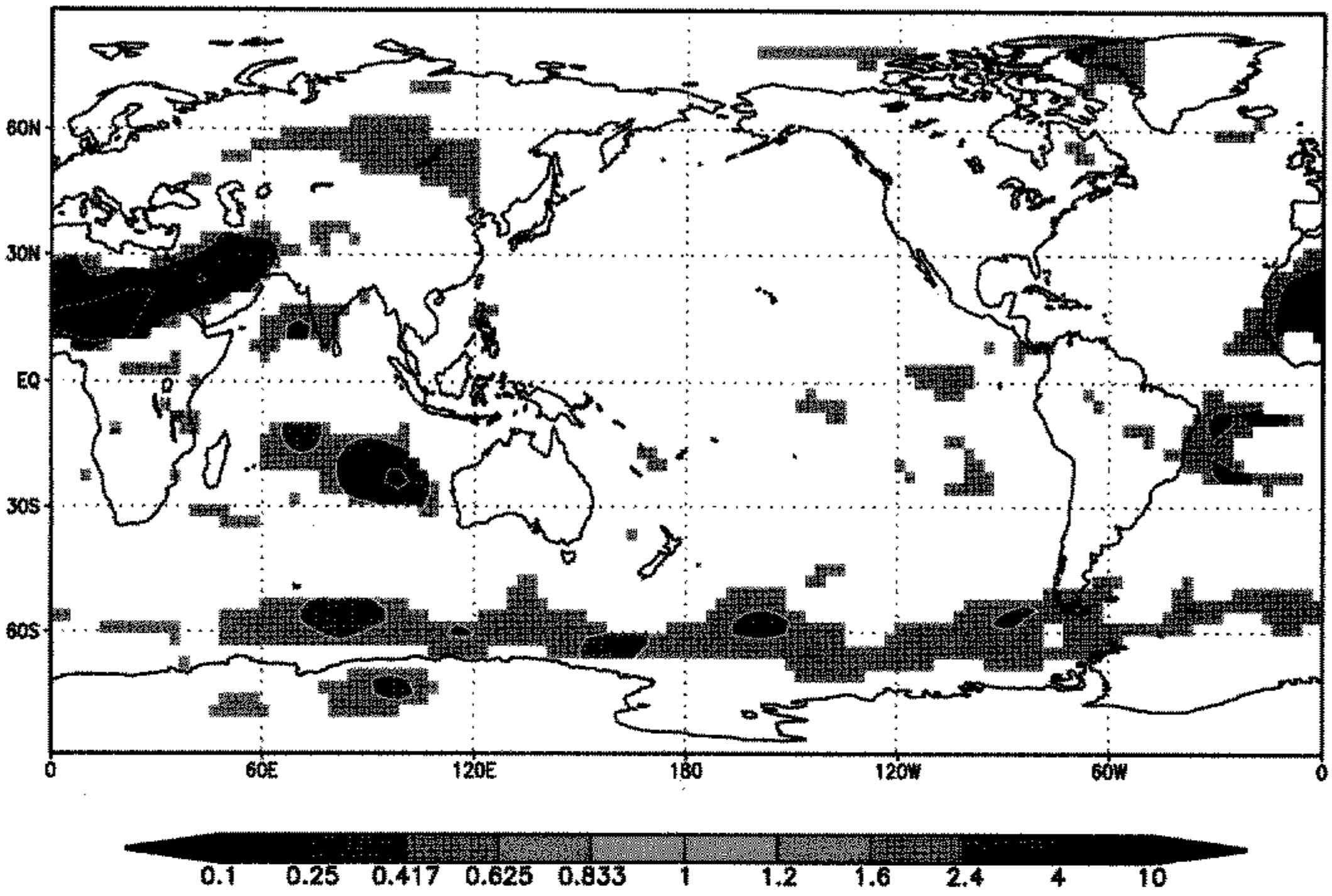

Figure 7. As Fig. 5 but for the 850 hPa mixing ratio.

(Fig. 3(a)) for the January mean difference. As the simulations proceed into February and March, differences in precipitation, soil moisture, and $q850$ are gradually reduced. In a given DSP ensemble member, this gradual equilibration toward the AMIP values occurs when occasional precipitation events lead to increased soil moisture and $q850$ (Fig. 8 shows hints of this behaviour; see below for discussion); this in turn tends to encourage more frequent precipitation events. The net result is that each DSP ensemble member undergoes a slow and sporadic drift towards the AMIP distribution. Differences in the mean are greatly reduced but not yet eliminated by March (Figs. 2(b), 3(b) and 4(b)).

The soil moisture ICs in all DSP ensemble members are identical, so the initial variance of the ensemble distribution is zero. By January, the initial soil moisture distribution over central Africa has spread out somewhat, but still has a variance much smaller than that of the AMIP ensembles (Fig. 5). The January DSP precipitation distribution also has much less variance than the AMIP ensembles (Fig. 6), as most of the DSP ensemble members have very little precipitation. Over the northern part of Africa and the Arabian peninsula, the variance of $q850$ is also greatly reduced (Fig. 7). In these areas, the lower atmosphere has been dessicated so that the ensemble distributions are squeezed tightly close to zero. However, in a smaller region over central Africa, the variance of $q850$ is actually greater in the DSP simulations. An examination of the details of the distribution at individual grid points shows that the $q850$ distributions are still not entirely dried out in the DSP ensemble. The distribution shape is similar to the shape of the distributions for the AMIP simulations, with the mean simply shifted to significantly lower values (Fig. 8). The variance is increased by a few DSP ensemble members (10 of 160) that have become much moister due to the chance occurrence of precipitation events, leading to a long positive tail for the DSP

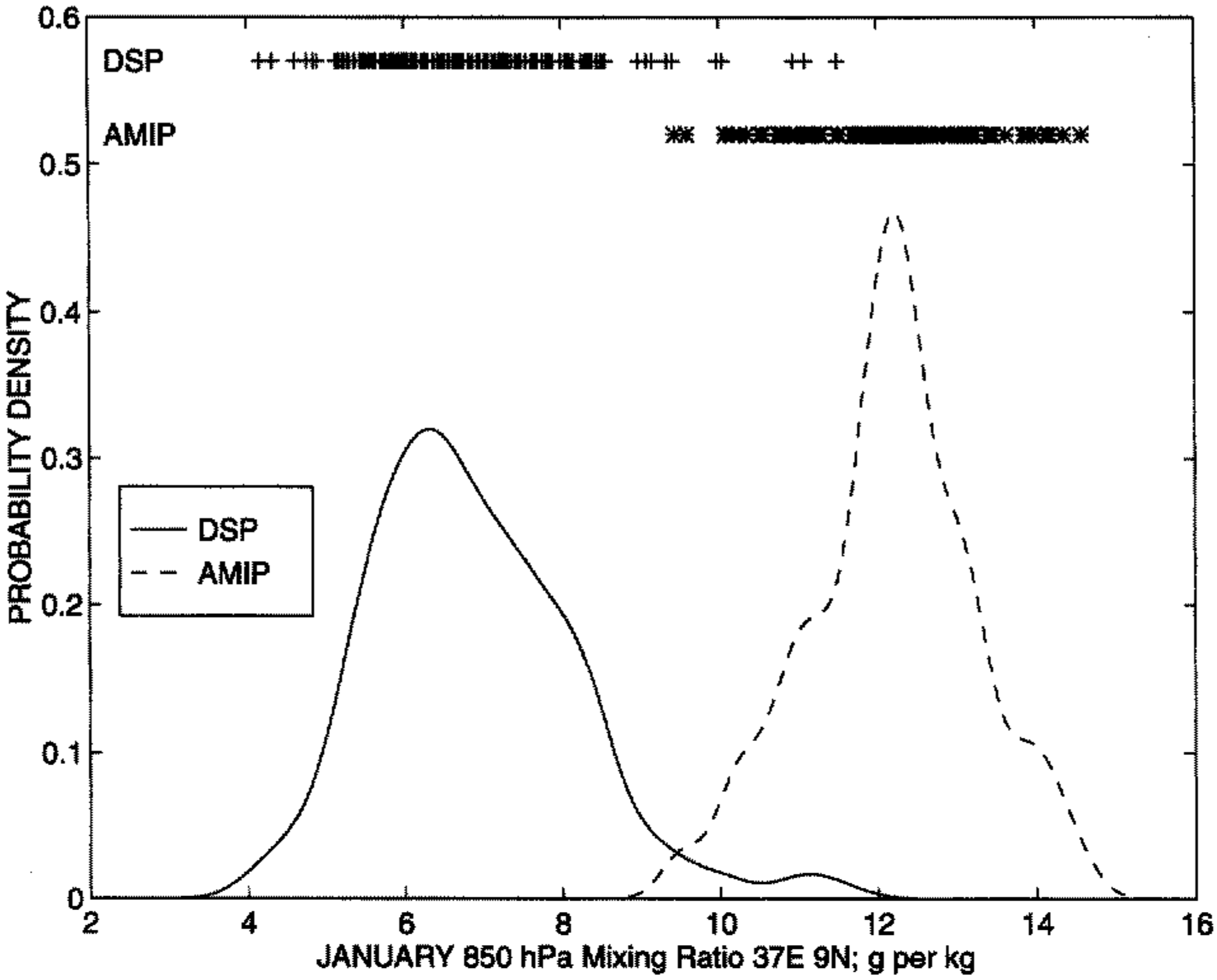

Figure 8. Distribution of Dynamical Seasonal Prediction (DSP) experiment and Atmospheric Model Intercomparison Project (AMIP) ensemble 850 hPa mixing ratio for January, for 1980–95 at 9°N, 37°E (marked by an asterisk in Fig. 3(a)) over central Africa. The solid (dashed) line shows a Gaussian kernel summation approximation of the probability distribution for the DSP (AMIP) ensemble, while the '+' and '*' show the values of the individual DSP and AMIP ensemble members, respectively.

$q850$ distributions. These $q850$ distributions are the first example of fields for which the DSP variance is larger than the AMIP variance, indicating that the introduction of ICs has reduced the potential predictability.

As forecast lead time increases through February and March, the variances of the DSP soil moisture and precipitation fields gradually widen, but they remain significantly less than the AMIP values through 3.5 months (not shown). The $q850$ variance-ratio patterns between DSP and AMIP simulations also stay much the same, but the mean differences gradually reduce in amplitude through February and March (not shown).

(*b*) *Australia, tropical Indian Ocean, and western tropical Pacific*

A second region of interest, over Australia and the surrounding waters of the tropical Indian Ocean and western tropical Pacific, contains the largest differences between the DSP and AMIP fields for precipitation. Changes in the rainfall distribution and the related large-scale circulation in this region appear to have profound effects on the global general circulation, but it is more difficult to assess the mechanism through which the changes are effected in this region.

Figure 2(a) shows that the DSP mean precipitation is significantly enhanced over western Australia and the Indian Ocean during January, but greatly reduced over the extreme western tropical Pacific to the north of Australia. The $q850$ is also significantly enhanced from western Australia west across the Indian Ocean (Fig. 3(a)), but shows a

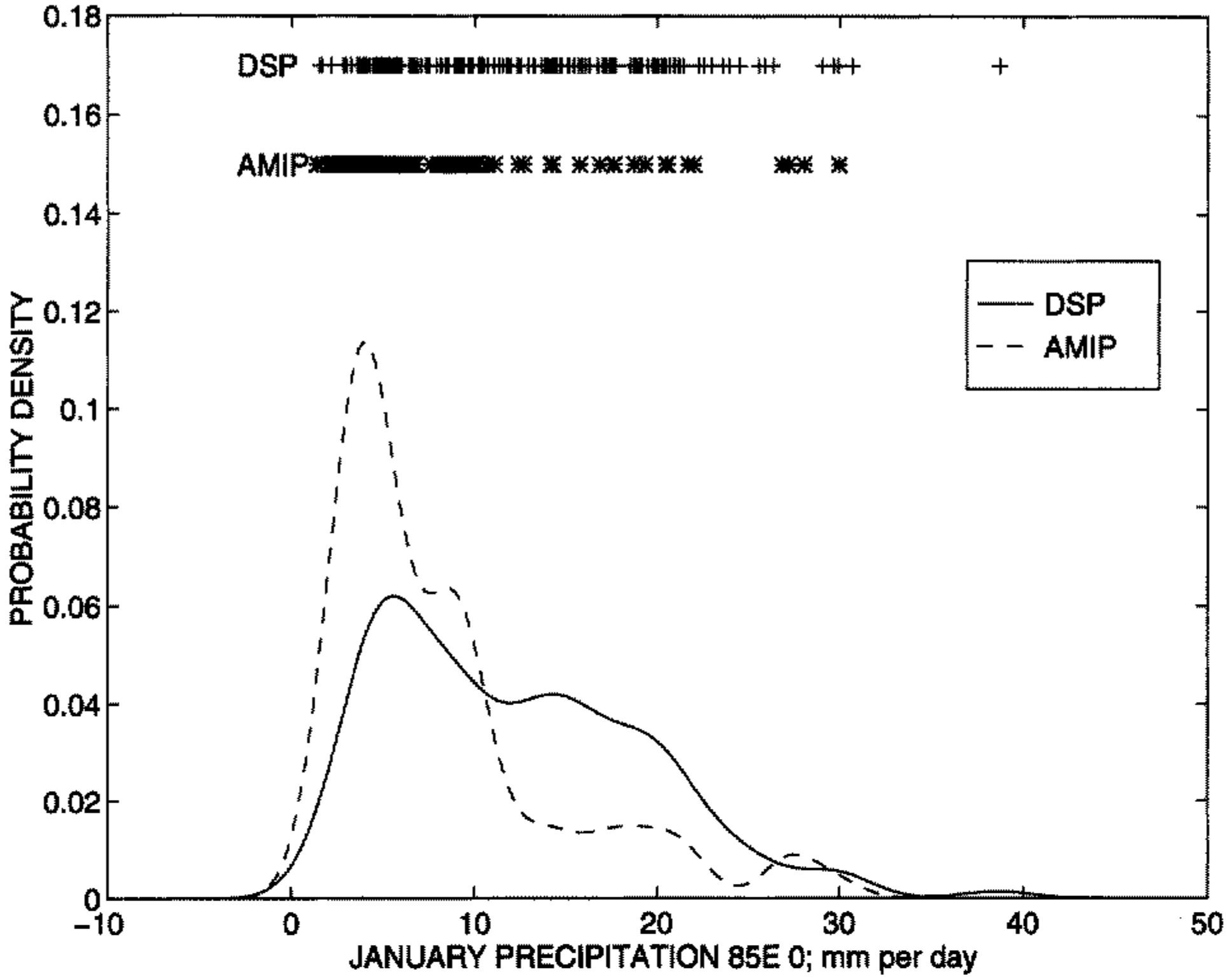

Figure 9. As Fig. 8 but for precipitation at 85°E and the equator (marked by the black asterisk in Fig. 2(a)) over the tropical Indian Ocean. The small non-zero probability of negative values is an artifact of the application of the kernel method for producing the continuous representation of the distribution.

much weaker reduction to the north of Australia. The DSP soil moisture ICs are wetter than the AMIP values over all but the east of Australia, but are much drier over some of the islands north of Australia and over south-east Asia (Fig. 1). These soil moisture differences are gradually reduced in January (Fig. 4(a)) and February and disappear almost entirely in March over Australia (Fig. 4(b)); they disappear more gradually over the areas north of Australia with significantly low soil moisture persisting through March. Precipitation and $q850$ differences are also gradually reduced in February and March, but are still quite large and significant in March (Figs. 2(b) and 3(b)).

The precipitation variance is much larger in the DSP simulations over western Australia and the Indian Ocean throughout all three months, and is smaller in regions to the north of Australia (Fig. 6). The ensemble distributions at many individual points show that this is primarily due to a larger positive tail in the precipitation distribution over Australia and the Indian Ocean (21% of DSP and 13% of AMIP simulations have more than 12 mm day^{-1}). Individual DSP ensemble members are more likely to be very wet over the Indian Ocean (Fig. 9), however, the majority of DSP members are not significantly wetter than the AMIP simulations. Precipitation variance is reduced to the north of Australia (Fig. 10), where the DSP distribution is relatively tightly constrained to values of precipitation that are much less than the AMIP mean. The AMIP distribution is broader and shifted to more positive values, with a long broad tail towards higher precipitation. The DSP distribution has only a handful of wet cases (only 20 of 160 are wetter than the AMIP mean), leading to a long but thin tail towards higher precipitation; the net result is much reduced variance for the DSP ensemble.

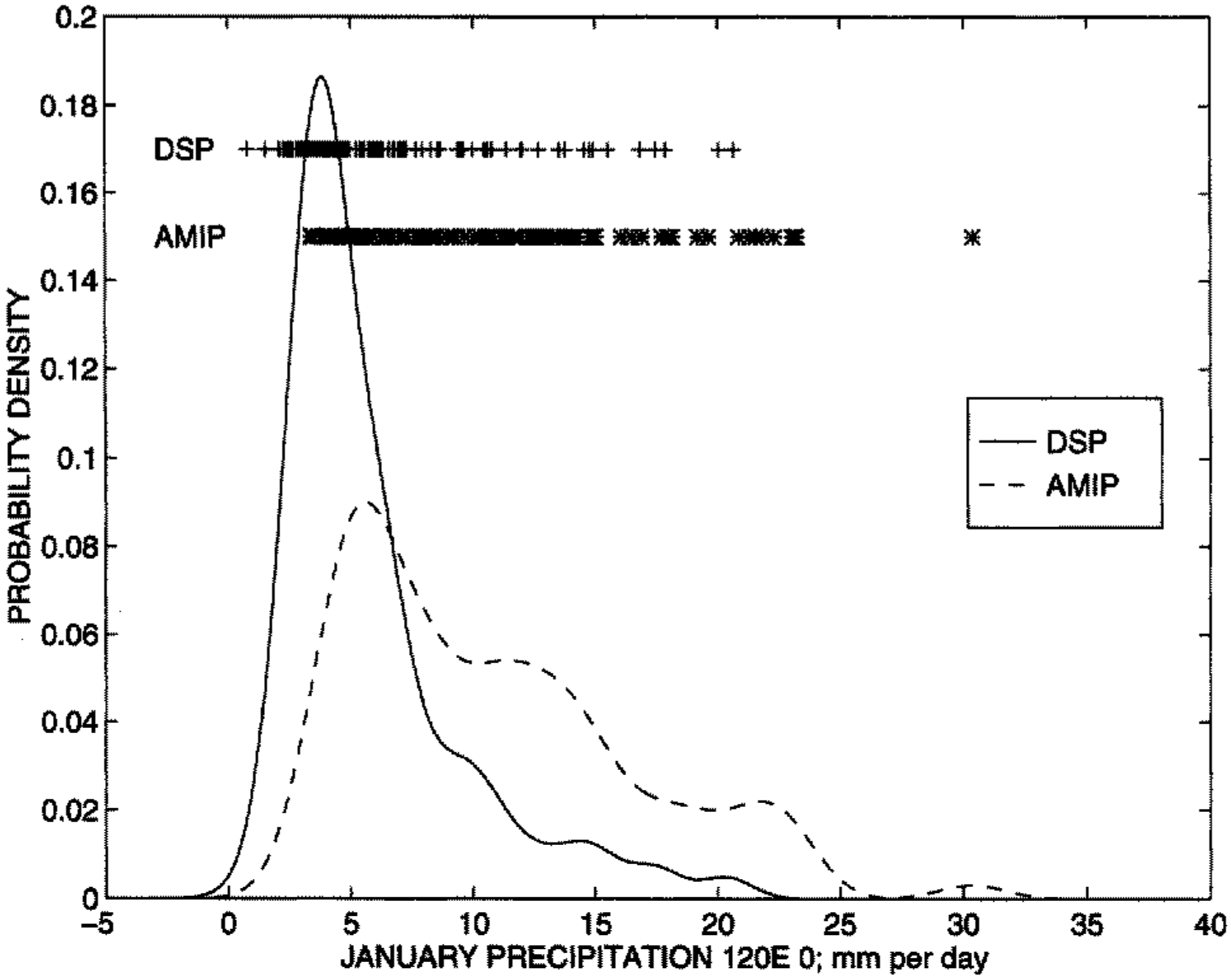

Figure 10. As Fig. 9 but for precipitation at 120°E and the equator (marked by the white asterisk in Fig. 2(a)) over Indonesia.

The DSP variance of $q850$ is substantially greater over parts of the Indian Ocean (Fig. 7). In general, this is consistent with the precipitation distribution in that there are a few DSP ensemble members that have significantly enhanced $q850$ in these regions (31 of 160 have $q850$ greater than that of the highest AMIP $q850$ at 25°S, 100°E in the area of the largest mean difference), while many other members look similar to the AMIP values. North of Australia, the complete $q850$ distributions are shifted to drier values with little change in variance; Fig. 7 shows only limited regions of significant variance differences north of Australia.

Soil moisture variance over Australia (Fig. 5 for January) is enhanced through all three months in the DSP runs. In most ensemble members, the DSP soil moisture here is very low, however, a limited number of members are much wetter, leading to a long positive tail on the distributions and a significant difference in the means. The opposite is seen north of Australia where a few of the DSP ensemble members have greatly reduced soil moisture, leading to greater variance (this is significant over Borneo and south-east Asia) and a significant difference in the mean.

It is very difficult to explain the differences between DSP and AMIP ensembles in this region as a direct local impact of land surface ICs. One could argue that the initially enhanced soil moisture in Australia can lead to enhanced low-level moisture being advected into the tropical Indian Ocean. Similarly, the limited land areas to the north of Australia can lead to drying of the lower atmosphere there in some ensemble members. The increased (decreased) lower-level moisture may lead to an increased (decreased) probability of strong convection over these regions. However, this behaviour does not appear to be taking place during the first few weeks of the DSP integrations.

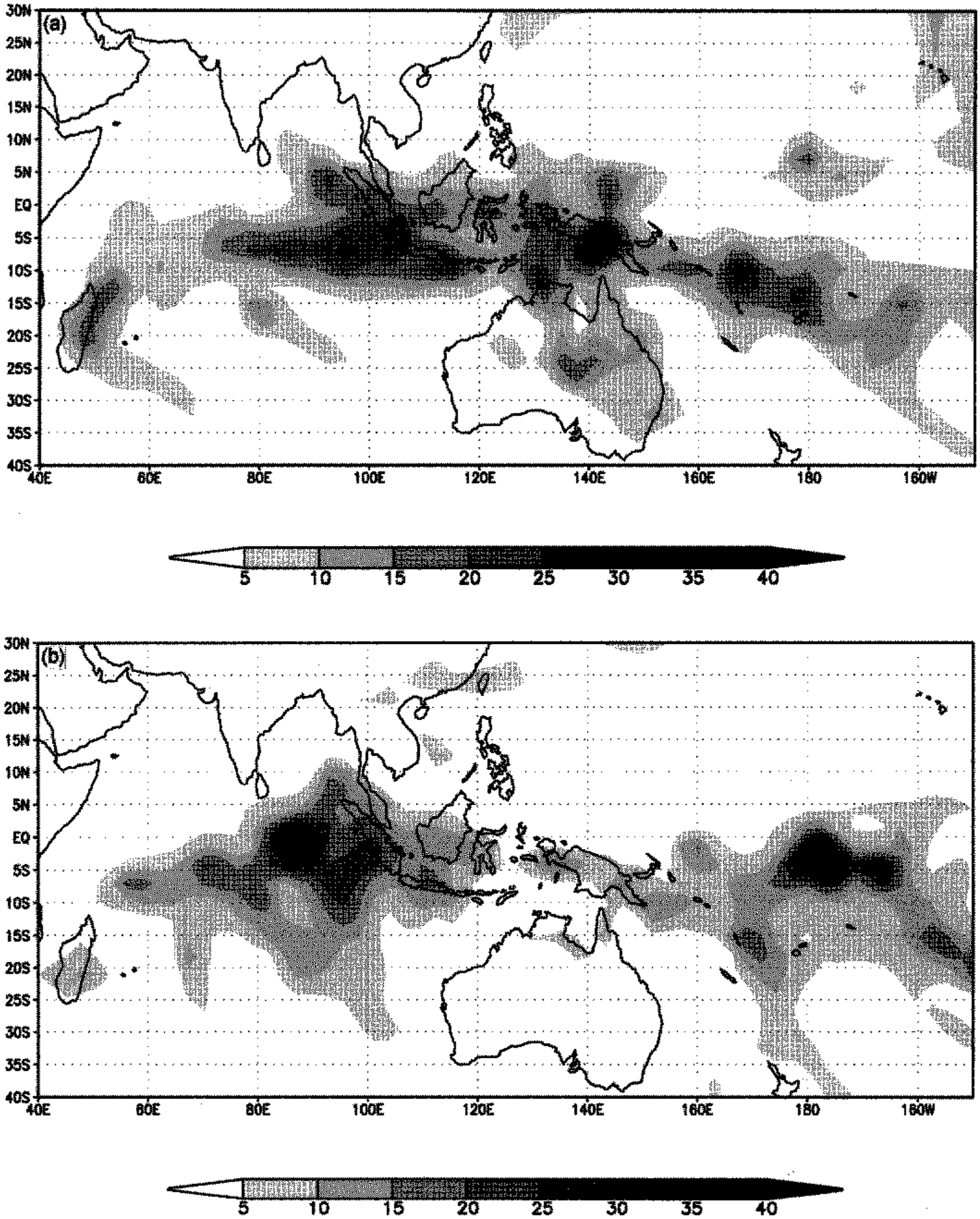

Figure 11. Monthly mean precipitation (mm day^{-1}) for January 1987, for: (a) Dynamical Seasonal Prediction (DSP) ensemble member 3, and (b) DSP member 9.

Furthermore, it seems unlikely that simple advection could explain such long-lasting differences over such large areas. Studies in regions with more land area have shown that such mechanisms can be important (Bosilovich and Sun 1999).

Increased precipitation over the Indian Ocean and decreased precipitation over the extreme western Pacific tend to occur together in the DSP ensembles, suggesting that a modification of the large-scale tropical circulation is playing a role here. Figure 11

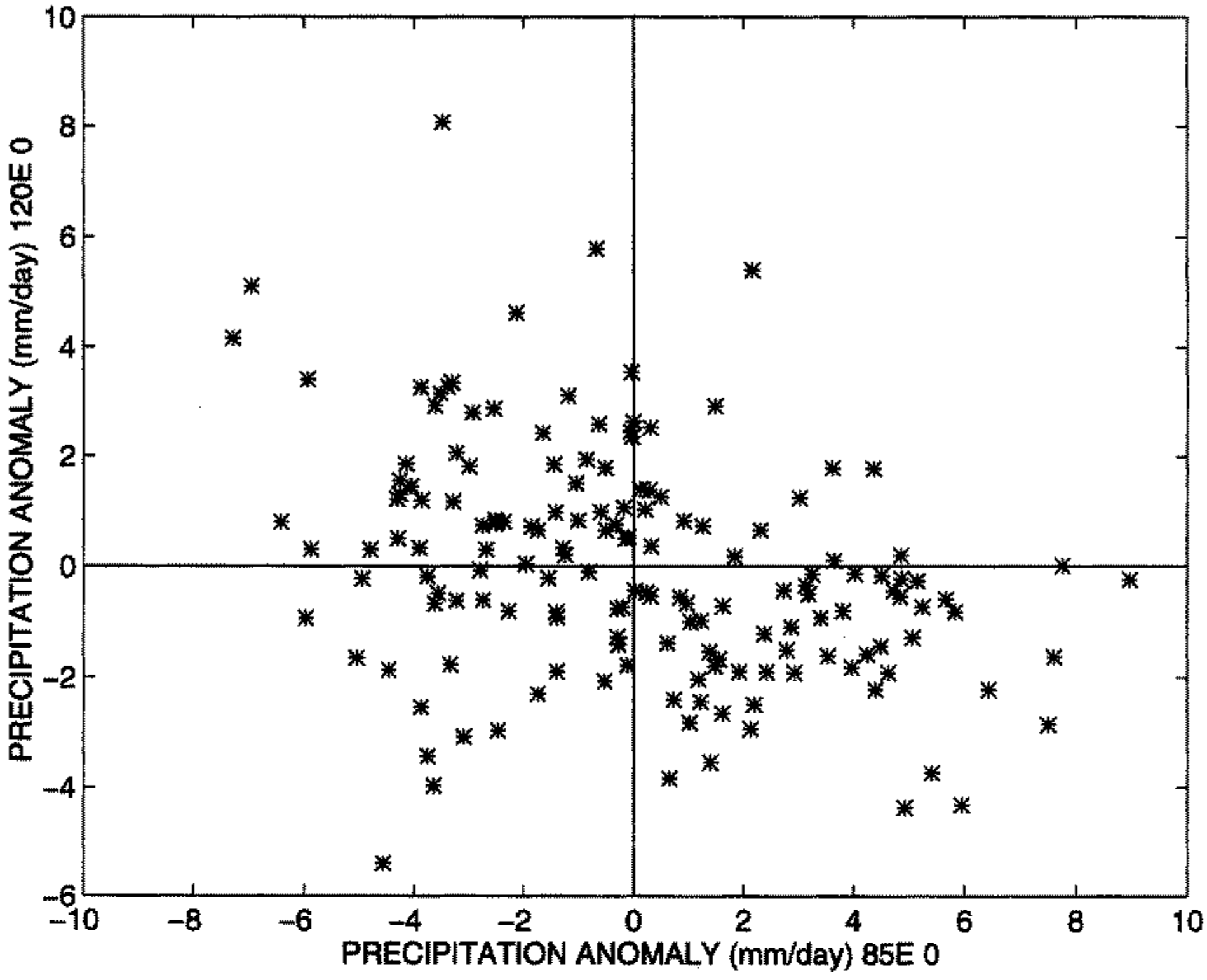

Figure 12. Scatter plot of Dynamical Seasonal Prediction anomalies of precipitation from the ensemble mean at 85°E and the equator, versus the anomalies at 120°E and the equator.

shows the precipitation patterns from two DSP ensemble members for 1987; the second member has much more Indian Ocean precipitation and less over the western Pacific. Figure 12 shows a scatter plot of the DSP precipitation anomalies from the ensemble mean for the points at the equator and 85°E, and the equator and 120°E (Figs. 9 and 10 show the distributions at these points); the correlation coefficient for these two distributions is −0.35. When a member of the DSP ensemble is dry (wet) in the tropical Indian Ocean it is likely to be wet (dry) in the western Pacific.

As noted above, this switch in precipitation centres takes place in a minority of DSP ensemble members (48 of 160 have precipitation greater than 10 mm day^{-1} at 85°E and the equator), and in an even smaller percentage of AMIP members (17 of 96). The result is still an enhanced DSP mean precipitation over the Indian Ocean, and an increased variance due to the long positive tail of the precipitation distribution in this region (Fig. 9). Again, the precipitation, $q850$, and soil moisture distributions tend to have increased variance in the DSP ensembles over much of this region, which might lead to the conclusion that the use of ICs is reducing potential predictability. The relative importance of the insertion of land surface and atmospheric ICs remains unclear in this analysis.

(*c*) *Eastern tropical Pacific*

Significant differences in mean precipitation (Fig. 2) and $q850$ (Fig. 3) between the DSP and AMIP simulations exist in the eastern tropical Pacific. This area includes much of the Niño-3 region (5°N–5°S, 150–90°W), which has been argued to be one of the most efficient areas in the tropics for exciting a northern hemisphere (NH)

extratropical response (Lau and Nath 1994; Trenberth *et al.* 1998). The DSP variance for precipitation (Fig. 6) is also larger than the AMIP variance in this region. There is significant interannual variability of both precipitation and $q850$ in both DSP and AMIP simulations associated with the El Niño Southern Oscillation (ENSO) variability that is part of the SST forcing; this interannual variability is roughly comparable in the DSP and AMIP ensembles. This is generally a very dry region in the model, with only 1983 (and to a lesser extent 1992) showing significant amounts of precipitation in most members of the ensembles. However, there are more cases in which a few of the DSP ensemble members are wet outliers (at 130°W on the equator, 7 of 160 DSP members and 2 of 96 AMIP members have precipitation exceeding 8 mm day^{-1}). This is reflected in the increase in the mean values and the variance of DSP precipitation. The wettest DSP cases are generally the same cases in which the precipitation is reduced over the western tropical Pacific Ocean. This suggests that a global modification to the tropical circulation is responsible for these precipitation changes, since there is no obvious local impact of differences in land surface ICs in the eastern tropical Pacific.

(*d*) *NH temperature regions*

In the NH, there are significant differences between the snow cover ICs for the DSP simulations and the climatological December mean snow cover of the AMIP simulations. The DSP ICs tend to have more snow that extends further south in regions that are not permanently snow covered. As noted in the next subsection, the DSP simulations tend to be colder at the surface than the AMIP simulations during January, so this snow cover difference is enhanced through January. Part of this reduced temperature is a direct impact of the greater regions of snow cover in the DSP runs, which lead to local cooling through enhanced surface albedo and the loss of heat needed to melt snow; this effect is not, however, entirely responsible for the NH cooling over land in the DSP simulations.

Although the DSP simulations start with no variance in snow cover by definition, variance grows rapidly during the first few weeks due to synoptic scale 'noise' that deposits snow in essentially random amounts and locations. The warmer AMIP simulations tend to have more precipitation events that are rain, and to have more regions where snow is absent in all ensemble members. The result is that large areas of the NH continents have a larger variance of snow cover in the DSP than in the AMIP simulations by January.

In February and especially in March snow begins to retreat northwards. This serves to accentuate the variance differences between the DSP and AMIP simulations, as more and more areas of the AMIP are snow free in most ensemble members while the DSP runs continue to have varying amounts of snowfall. This enhanced DSP snow cover variability leads directly to large variability in the surface temperature, which is seen over significant portions of the NH mid-latitude land surface during March.

(*e*) *Extratropical hemispheric differences*

There are significant differences in the interhemispheric distribution of temperature/mass between the DSP and AMIP ensembles; this appears to be in contrast to results obtained by Wang and Kumar (1998), who found little impact from land surface ICs away from the surface in AGCM experiments. During the first few weeks of the DSP integrations the NH cools at all levels from the surface to 300 mb, with the largest cooling in the lower troposphere. Since SSTs are prescribed, the surface cooling is confined to continental regions, while cooling aloft is more homogeneous throughout

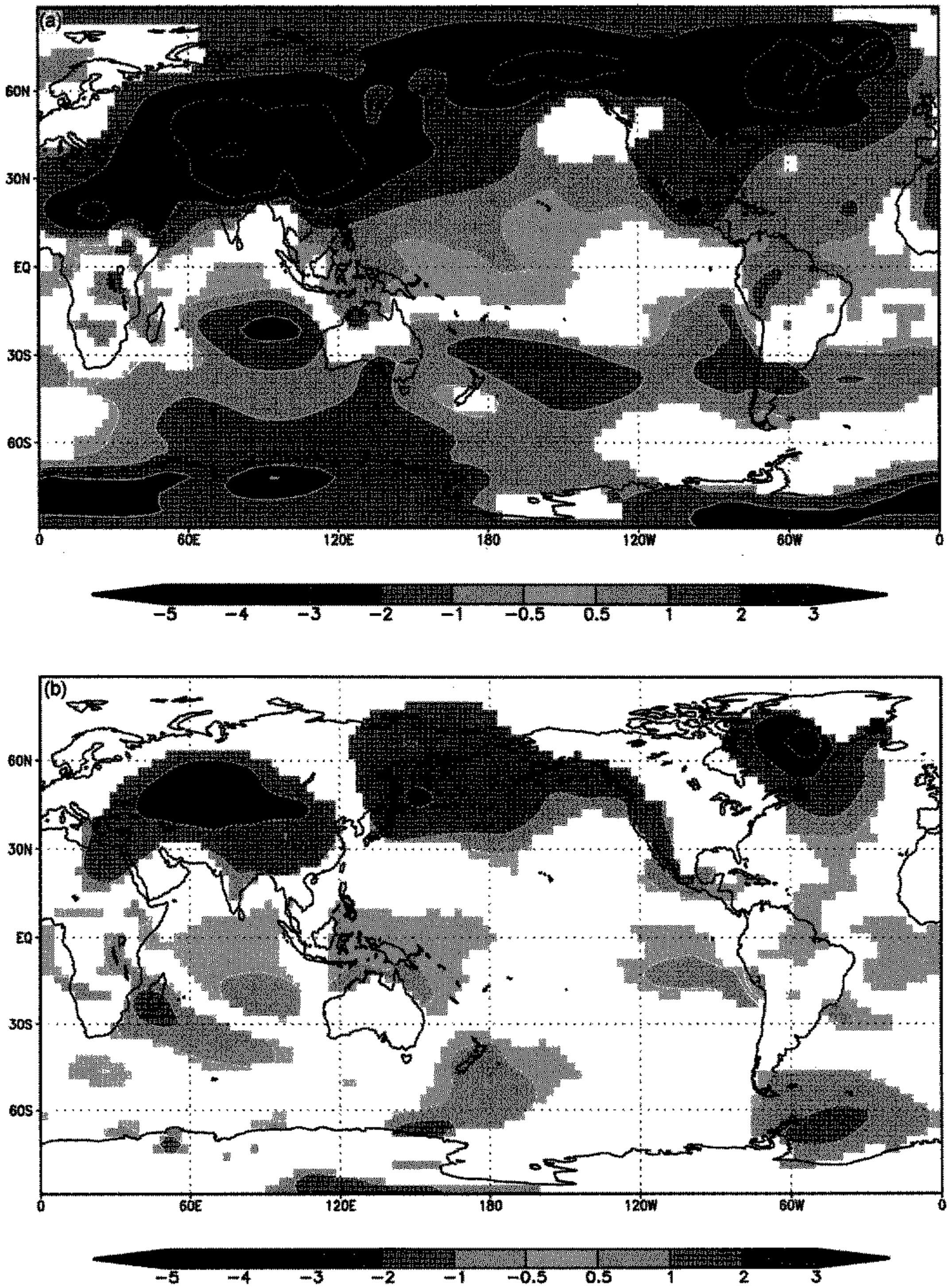

Figure 13. As Fig. 2 but for 850 hPa temperature (degC).

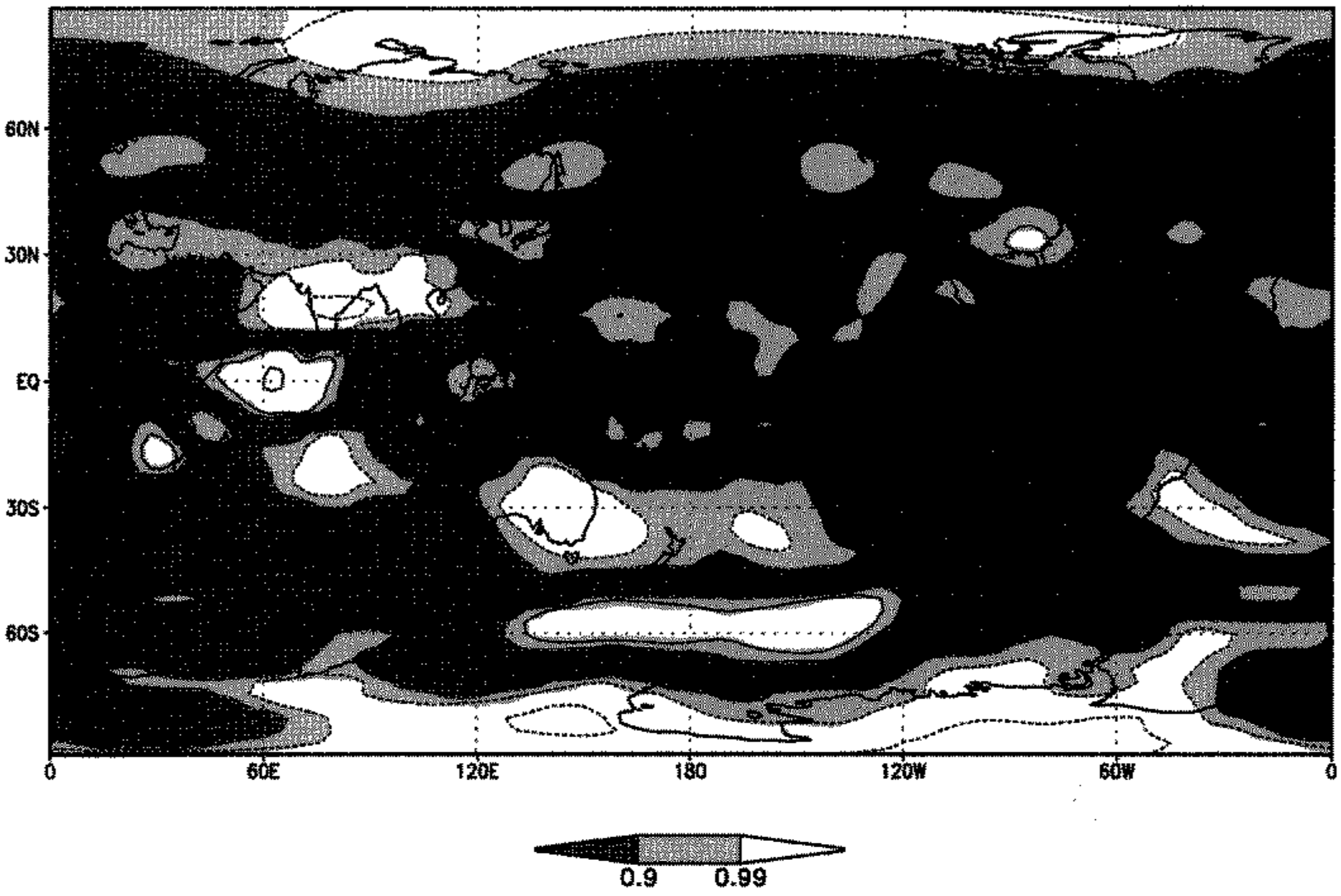

Figure 14. Ratio of Dynamical Seasonal Prediction to Atmospheric Model Intercomparison Project variance of 200 hPa temperature around the corresponding ensemble mean (internal variance; see text for details) for January. Contours are at 1.2, 1.6, 2.4, 4.0, 10.0 and the reciprocals of these values; contours less than unity are dashed. Regions where an f-test indicates that the difference in variance is significant at greater than 99%, greater than 90% (but less than 99%) or less than 90% confidence are unshaded, lightly shaded or heavily shaded, respectively.

the hemisphere in January (Fig. 13(a)). In the southern hemisphere a small warming at the surface increases with height, however, the magnitude of the warming is much less than that in the NH. The difference between DSP and AMIP temperatures decreases with forecast lead time, and has been greatly reduced above the surface by March (Fig. 13(b)). This hemispheric temperature decrease in the NH also leads to a hemispheric decrease in atmospheric water vapour as seen for January in Fig. 3(a). This decrease is small compared with the regional signals discussed in earlier subsections, and it also mostly disappears by March (Fig. 3(b)). The variance of the temperature (and height/pressure) and the water vapour fields do not show a hemispheric pattern, as this is primarily a shift of the entire ensemble distribution without changing its shape. The exact cause of this initial NH cold shift in the DSP ensembles is not fully understood, but will be the subject of further investigation.

Although the hemispheric cooling does not impact the variance in the NH extra-tropics, Fig. 14 does show some intriguing differences between the DSP and AMIP variance for the 200 hPa temperature field for January. Regions of greater variance in the DSP ensemble appear to correspond with the traditional centre of the Pacific–North American (PacNA) pattern. Although only one of the centres, over the south-east USA, appears with greater than 99% confidence, two other centres over the Gulf of Alaska and the upper midwest appear with confidence greater than 90%. Similar results are seen for tropospheric height patterns. Figure 6 shows that precipitation variance in the tropics is increased over large parts of the Indian Ocean and the eastern tropical Pacific in the DSP ensembles. These regions of tropical convection, in particular the eastern

tropical Pacific, are known to have impacts on the strength of this model's PacNA pattern (Trenberth *et al.* 1998), consistent with many other models and the observed atmosphere. Apparently, increased DSP variance in convection in these regions also leads to increased variance in the PacNA response. This leads to reduced estimates of potential predictability for the PacNA region for the DSP simulations which make use of ICs.

4. Discussion

(*a*) *Impact of ICs on ensemble mean predictions*

The DSP and AMIP simulations can be viewed in an idealized sense as two ways of making a seasonal prediction assuming, of course, that SSTs can be predicted perfectly up to three months in advance. While this is not the case, the slow time-scale of evolution for anomalous SSTs, especially in the tropics, facilitates highly accurate SST predictions one month in advance, and reasonably accurate predictions out to at least three months in many cases.

Given this caveat on SSTs, the AMIP simulations can be viewed as seasonal forecasts, in which no information from atmosphere or land surface observations is used (consistent with this paradigm, the simulations are referred to as forecasts in this section). The DSP forecasts assume that the observed state of the atmosphere is represented by the NCEP re-analyses. The DSP forecasts also assume that there exist complete accurate observations of the soil moisture and snow cover, these observations being the same each year and coming from the climatological distributions of a long run of a previous version of the AGCM. The DSP seasonal predictions are produced by integrating the AGCM forward from these 'observed' ICs.

The previous section examined some of the differences between the AMIP forecasts and the DSP forecasts. The ICs led to large changes in the tropical precipitation distribution and in the statistics of the entire tropical circulation. There were also regional direct impacts of the land surface ICs, most notably over Africa and in snow covered regions of the NH mid latitudes. Large-scale extratropical impacts include temperature changes in the lower levels of the troposphere, especially over the continents. In this experimental design it is not possible to say whether the impact of ICs has improved the quality of the seasonal forecasts (since the observed land surface conditions come from a model climatology while the atmospheric ICs come from an analysis of the observed atmosphere). Nevertheless, it seems fair to assume that adding good ICs in DSP should tend to improve forecasts in comparison with the AMIP forecasts.

However, there are a number of examples where inserting 'unbalanced' observations taken from a numerical model into that same model can lead to an initial period of error growth, sometimes referred to as IC shock or 'spin-up error' (Miyakoda *et al.* 1978). Simple examples of this phenomena occur in low-order models that are used for theoretical predictability studies; for instance, the three-variable model of Lorenz (1963) which is shown to undergo transient initial-error growth by Anderson and Hubeny (1997). Primitive-equation models of the atmosphere, ranging from the highly truncated 9-variable model of Lorenz (1980) through full dry atmospheric GCMs, display an approximately balanced flow when integrated over long periods of time. Again, when imperfect observations taken from these models are inserted into the models, a period of transient error growth, characterized by large-amplitude gravity waves, occurs (Vautard and Legras 1986; Anderson and Hubeny 1997). Other more subtle balances also exist in AGCMs. For instance, Anderson and van den Dool (1993) showed a period of transient error growth in the statistics of atmospheric blocking in integrations of an AGCM starting from observed atmospheric ICs. There are most likely to be a number

of other balances that exist in AGCMs that can be destroyed by introducing observed atmospheric states, independent of the land surface state.

In the DSP forecasts examined here it is still not clear just how large the IC shock error growth is. If this growth is large, it is not inconceivable that forecasts made using (accurately) observed land surface ICs could lead to forecasts that are worse than those made in AMIP forecasts with no ICs. Insufficient evidence is presented here to advocate strongly for this possibility, but neither can it be ruled out.

A caveat applies to these results due to slight differences in the DSP and AMIP SST forcing, as noted in section 2. While these differences in SST are generally very small, especially in the tropics from whence most of the impact of SST forcing is expected to originate, they might still have some impact on the different mean responses of the DSP and AMIP ensembles. However, there is evidence that the SST differences are not responsible for the results discussed in section 3. First, for 1980 and 1981 the SSTs in the two cases are almost identical, and these two years seem to demonstrate the same behaviour as the longer 16-year period. Second, a single AMIP simulation from 1979 to 1995 has been created with SSTs that are almost identical to the SSTs used in the DSP simulations. This single AMIP simulation appears to be consistent with the other AMIP ensemble members and an outlier from the DSP ensemble members, for quantities such as soil moisture, atmospheric moisture content, precipitation, snow cover and hemispheric temperature distribution that were examined in section 3.

(*b*) *Impacts of ICs on potential predictability*

Section 3 also examined the impact of ICs on the internal variance of the ensemble forecast distributions, a quantity related to most common measures of potential predictability. Naively, one would assume that inserting observations of land surface processes with no IC variance (delta function distributions) would not lead to higher variance (and consequently lower potential predictability) for DSP fields, and might be expected to lead to reduced variance in the mean. For short DSP forecasts out to a few days this is true, but the distributions of many model quantities, especially those related to hydrologic processes, rapidly spread out as the forecast lead grows. Results presented here suggest that for many atmospheric variables the variance is increased by the insertion of the ICs. When producing real forecasts behaviour like this could lead to the counter-intuitive result of reduced estimates of potential predictability (and possibly reduced forecast skill) when using IC information.

(*c*) *Implications for coupled model seasonal prediction*

True seasonal predictions by numerical models are generally made by two-tiered forecast systems, in which the second tier is essentially identical to the DSP-type simulations described here (Ji *et al.* 1998; Latif *et al.* 1998). Work is also ongoing on the development of fully coupled ocean–atmosphere GCMs for seasonal prediction (Stockdale *et al.* 1998; Yang *et al.* 1998). These fully coupled models tend to have huge initial drift, and a variety of IC shocks related to the insertion of observed ocean data into the coupled GCM (Rosati *et al.* 1997; Yang *et al.* 1998). Using observed ICs for the land surface and the atmosphere has potential to introduce even more problems, consistent with the results for AGCMs presented here.

Given that land surface data are sparse, and in some instances of questionable quality, it is unlikely that observed ICs for land surface variables would be more consistent with a GCM than is the case in the DSP experiments here, where the ICs come from another version of the same AGCM. Hence, it is possible that even bigger IC

shocks could be associated with introducing observed land surface ICs into second-tier AGCM or fully coupled GCM forecasts. To reduce this type of IC shock fully coupled assimilation systems may be necessary, along with methods for reducing imbalances that may occur in assimilated ICs (Larow and Krishnamurti 1998). Of course, improving models to be more consistent with the real world should also help in the long run. Until progress can be made on land surface data availability and assimilation (Houser *et al.* 1999), coupled assimilation, and model improvement, one must consider carefully whether introducing observed ICs for various components of AGCMs will have a positive impact on seasonal-forecast quality.

5. Conclusions

AGCM seasonal simulations from the DSP experiment have been compared with long AMIP simulations using the same AGCM; both simulations are forced by observed SSTs. The ICs for the DSP simulations are taken from observations for the atmosphere, and from the climatology of a previous version of the AGCM for snow and soil moisture. Differences between ensembles of DSP and AMIP integrations can be used to simulate the impacts of using ICs on seasonal lead predictions. Large and significant differences in the DSP and AMIP fields are found throughout the 3.5-month DSP simulations; differences are found in both the ensemble-mean quantities and in the variance of the ensembles. In many cases, especially for fields related directly to hydrological processes, the internal variance of the DSP simulations is found to exceed that of the AMIP simulations. This leads to the somewhat counter-intuitive conclusion that the introduction of IC information can lead to a reduction in estimates for the potential predictability. Although the relative errors of ensemble-mean values cannot be evaluated in this experimental design, it seems likely that effects of introducing IC information for the land surface and atmosphere might actually also reduce the skill of seasonal simulations in some cases. This is interpreted as being the results of initial-error growth due to the shock of inserting observed ICs into a model with a climatology inconsistent with these observations. The results suggest that one must carefully evaluate the efficacy of using ICs when making seasonal predictions with AGCMs or coupled GCMs.

Acknowledgements

This research would not have been possible without the assistance of Matt Harrison, Anthony Rosati, Rich Gudgel, Joe Sirutis, Xiu-Qun Yang, Bob Smith, Tony Gordon, Bill Stern and Bruce Wyman who all helped in the design, implementation, and production of the GFDL seasonal-prediction system. Two anonymous reviewers provided many helpful comments that significantly improved this manuscript.

References

Anderson, J. L. 1996 A method for producing and evaluating probabilistic forecasts from ensemble model integrations. *J. Climate*, **9,** 1518–1530

Anderson, J. L. and Stern, W. F. 1996 Evaluating the potential predictive utility of ensemble forecasts. *J. Climate*, **9,** 260–269

Anderson, J. L. and Hubeny, V. 1997 A reexamination of methods for evaluating the predictability of the atmosphere. *Nonlinear Processes in Geophys.*, **4,** 157–165

Anderson, J. L. and van den Dool, H. M. 1993 The climatology of blocking in a numerical forecast model. *J. Climate*, **6,** 1041–1056

Barker, T. W. 1991 The relationship between spread and forecast error in extended-range forecasts. *J. Climate*, **4,** 733–742

Barsugli, J. J., Whitaker, J. S., Loughe, A. F. and Sardeshmukh, P. 1999 Effect of the 1997–98 El Niño on individual large-scale weather events. *Bull. Am. Meteorol. Soc.*, **80,** 1399–1411

Bosilovich, M. G. and Sun, W.-Y. 1999 Numerical simulation of the 1993 midwestern flood: Land–atmosphere interactions. *J. Climate*, **12,** 1490–1505

Branković, Č., Palmer, T. N. and Ferranti, L. 1994 Predictability of seasonal atmospheric variations. *J. Climate*, **7,** 217–237

Buizza, R. and Palmer, T. N. 1998 Impact of ensemble size on ensemble prediction. *Mon. Weather Rev.*, **126,** 2503–2518

Carson, D. J. 1998 Seasonal forecasting. *Q. J. R. Meteorol. Soc.*, **124,** 1–26

Chen, W. Y. and van den Dool, H. M. 1997 Atmospheric predictability of seasonal, annual, and decadal climate means and the role of the ENSO cycle: A model study. *J. Climate*, **10,** 1236–1254

Crutcher, H. L. and Meserve, M. 1970 *Selected-level heights, temperature and dewpoint temperatures for the northern hemisphere*. Naval Weather Service Command, Govt. Printing Office, Washington DC, USA

Deardorf, J. W. 1978 Efficient prediction of ground surface temperature and moisture, with inclusion of a layer of vegetation. *J. Geophys. Res.*, **83,** 1889–1903

Delsol, F., Miyakoda, K. and Clarke, R. H. 1971 Parameterized processes in the surface boundary layer of an atmospheric circulation model. *Q. J. R. Meteorol. Soc.*, **97,** 181–208

Derber, J. and Rosati, A. 1989 A global oceanic data assimilation system. *J. Phys. Oceanogr.*, **19,** 1333–1347

Ebisuzaki, W. 1995 The potential predictability in a 14-year GCM simulation. *J. Climate*, **8,** 2749–2761

ECMWF 1988 *Research Manual 3, ECMWF forecast model, physical parameterisation, 3rd Edition*. Ed. J.-F. Louis. ECMWF Research Dept., Shinfield Park, Reading, UK

Gates, W. 1992 AMIP: The Atmospheric Model Intercomparison Project. *Bull. Am. Meteorol. Soc.*, **73,** 1962–1970

Gordon, C. T. 1992 Comparison of 30-day integrations with and without cloud–radiation interaction. *Mon. Weather Rev.*, **120,** 1244–1277

Gordon, C. T. and Stern, W. F. 1982 A description of the GFDL global spectral model. *Mon. Weather Rev.*, **110,** 625–644

Graham, R. J., Evans, A. D. L., Mylne, K. R., Harrison, M. S. J. and Robertson, K. B. 2000 An assessment of seasonal predictability using atmospheric general circulation models. *Q. J. R. Meteorol. Soc.*, **126,** 2211–2240

Houser, P. R., Shuttleworth, W. J., Famiglietti, J. S., Gupta, H. V., Syed, K. H. and Goodrich, D. C. 1999 Integration of soil moisture, remote sensing and hydrologic modeling using data assimilation. *Weather Resour. Res.*, **34,** 3405–3420

Ji, M., Behringer, D. W. and Leetmaa, A. 1998 An improved coupled model for ENSO prediction and implications for ocean initialization. Part II: The coupled model. *Mon. Weather Rev.*, **126,** 1022–1034

Larow, T. E. and Krishnamurti, T. N. 1998 Initial conditions and ENSO prediction using a coupled ocean–atmosphere model. *Tellus*, **50A,** 76–94

Latif, M., Anderson, D., Barnett, T., Cane, M., Kleeman, R., Leetmaa, A., O'Brien, J., Rosati, A. and Schneider, E. 1998 A review of the predictability and prediction of ENSO. *J. Geophys. Res.*, **103,** 14375–14393

Lau, N. C. and Nath, M. J. 1994 A modeling study of the relative roles of tropical and extratropical SST anomalies in the variability of the global atmosphere–ocean system. *J. Climate*, **7,** 1184–1207

Livezey, R. E., Masutani, M. and Ji, M. 1996 SST-forced seasonal simulation and prediction skill for versions of the NCEP/MRF model. *Bull. Am. Meteorol. Soc.*, **77,** 507–517

Lorenz, E. N. 1963 Deterministic nonperiodic flows. *J. Atmos. Sci.*, **20,** 130–141

1980 Attractor sets and quasi-geostrophic equilibrium. *J. Atmos. Sci.*, **37,** 1685–1699

Miyakoda, K., Strickler, R. F. and Chludzinski, J. 1978 Initialization with the data assimilation method. *Tellus*, **30,** 32–54

Mo, K. C. and Kalnay, E. 1991 Impact of sea surface temperature anomalies on the skill of monthly forecasts. *Mon. Weather Rev.*, **119,** 2771–2793

Navarra, A., Stern, W. F. and Miyakoda, K. 1994 Reduction of Gibbs oscillation in spectral model simulation. *J. Climate*, **7,** 1169–1183

Nogues-Paegle, J., Rodgers, D. A. and Mo, K. C. 1992 Low-frequency predictability of the Dynamical Extended-Range Forecast Experiment. *Mon. Weather Rev.*, **120,** 2025–2041

Palmer, T. N., Branković, Č and Richardson, D. S. 2000 A probability and decision-model analysis of PROVOST seasonal multi-model ensemble integrations. *Q. J. R. Meteorol. Soc.*, **126,** 2013–2033

Press, W. R., Flannery, B. P., Teulosky, S. A. and Vetterling, W. T. 1986 *Numerical recipes: The art of scientific computing.* Cambridge University Press, Cambridge, UK

Reynolds, R. W. and Smith, T. M. 1994 Improved global sea surface temperature analyses using optimum interpolation. *J. Climate*, **7,** 929–948

Rosati, A., Gudgel, R. and Miyakoda, K. 1995 Decadal analysis produced from an ocean data assimilation system. *Mon. Weather Rev.*, **123,** 2206–2228

Rosati, A., Miyakoda, K. and Gudgel, R. 1997 The impact of ocean initial conditions on ENSO forecasting with a coupled model. *Mon. Weather Rev.*, **125,** 754–772

Rowell, D. P. 1998 Assessing potential seasonal predictability with an ensemble of multidecadal GCM simulations. *J. Climate*, **11,** 109–120

Schar, C., Luthi, D., Beyerle, U. and Erdmann, H. 1999 The soil-precipitation feedback: A process study with a regional climate model. *J. Climate*, **12,** 722–741

Shukla, J., Anderson, J., Baumhefner, D., Branković, Č., Chang, Y., Kalnay, E., Marx, L., Palmer, T. N., Paolino, D., Ploshay, J., Schubert, S., Straus, D., Suarez, N. and Tribbia, J. 2000 Dynamical seasonal prediction. *Bull. Am. Meteorol. Soc.*, in press

Sirutis, J. and Miyakoda, K. 1990 Subgrid scale physics in 1-month forecasts. Part I: Experiment with four parameterization packages. *Mon. Weather Rev.*, **118,** 1043–1064

Stern, W. F. and Miyakoda, K. 1989 'Systematic errors in GFDL's extended range prediction spectral GCM'. Pp. 136–140 in Proceedings of the ICSU/WMO workshop on systematic errors in models of the atmosphere. WMO TD No. 273, World Meteorological Organization, Geneva, Switzerland

1995 Feasibility of seasonal forecasts inferred from multiple GCM simulations. *J. Climate*, **8,** 1071–1085

Stockdale, T. N., Anderson, D. L. T., Alves, J. O. S. and Balmaseda, M. A. 1998 Global seasonal rainfall forecasts using a coupled ocean–atmosphere model. *Nature*, **392,** 370–373

Tracton, M. S. and Kalnay, E. 1993 Operational ensemble prediction at the National Meteorological Center: practical aspects. *Weather and Forecasting*, **8,** 379–398

Trenberth, K. E., Branstator, G. W., Karoly, D., Kumar, A., Lau, N. C. and Ropelewski, C. 1998 Progress during TOGA in understanding and modeling global teleconnections associated with tropical sea surface temperatures. *J. Geophys. Res.*, **103,** 14291–14324

Vautard, R. and Legras, B. 1986 Invariant manifolds, quasi-geostrophy and initialization. *J. Atmos. Sci.*, **43,** 565–584

Vinnikov, K. Y., Robock, A., Qiu, S., Entin, J. K., Owe, M., Choudhury, B. J., Hollinger, S. E. and Njoku, E. G. 1999 Satellite remote sensing of soil moisture in Illinois, United States. *J. Geophys. Res.*, **104,** 4145–4168

Wang, W. and Kumar, A. 1998 A GCM assessment of atmospheric seasonal predictability associated with soil moisture anomalies over North America. *J. Geophys. Res.*, **103,** 28637–28646

White, G. H., Kalnay, E., Gardner, R. and Kanamitsu, M. 1993 The skill of precipitation and surface temperature forecasts by the NMC global model during DERF II. *Mon. Weather Rev.*, **121,** 805–814

Wittrock, V. and Ripley, E. A. 1999 The predictability of autumn soil moisture levels on the Canadian Prairies. *Int. J. Climatol.*, **19,** 271–289

Wobus, R. L. and Kalnay, E. 1995 Three years of operational prediction of forecast skill at NMC. *Mon. Weather Rev.*, **123,** 2132–2148

Yang, X.-Q., Anderson, J. L. and Stern, W. F. 1998 Reproducible forced modes in AGCM ensemble integrations and potential predictability of atmospheric seasonal variations in the extratropics. *J. Climate*, **11,** 2942–2959